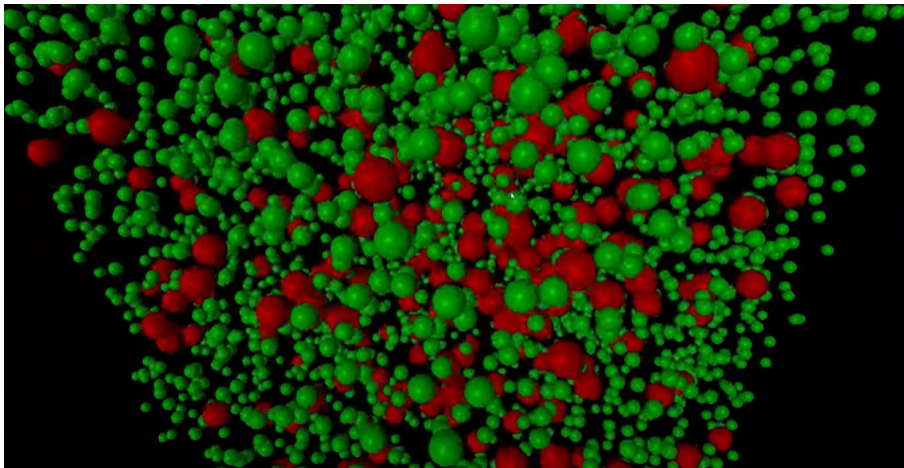


## Assignment 1

Computational Physics - FY8904

# Event-driven simulation of a two-dimensional gas



<https://compphys.go.ro/event-driven-molecular-dynamics/>

**Author:**  
Sam Narimani

May, 2023

---

# Table of Contents

<b>List of Figures</b>	<b>i</b>
<b>List of Tables</b>	<b>i</b>
<b>1 Introduction</b>	<b>1</b>
<b>2 Code framework</b>	<b>1</b>
<b>3 Simulation results</b>	<b>1</b>
3.1 Problem 1 . . . . .	1
3.2 Problem 2 . . . . .	2
3.3 Problem 3 . . . . .	7
3.4 Problem 4 . . . . .	8
<b>Bibliography</b>	<b>10</b>
<b>Appendix</b>	<b>11</b>
A Code structure . . . . .	11

## List of Figures

1	Velocity distribution 40k collisions - 2k particles . . . . .	2
2	Velocity distribution 40k collisions - 4k particles . . . . .	3
3	Maxwell-Boltzmann distribution . . . . .	4
4	Velocity distribution 60k collisions - 4k particles for . . . . .	5
5	Velocity distribution 60k collisions - 4k particles for . . . . .	6
6	$\zeta = 1$ . . . . .	7
7	$\zeta = 0.9$ . . . . .	8
8	$\zeta = 0.8$ . . . . .	8
9	$h_{crater}$ . . . . .	9

## List of Tables

1	Average velocity and kinetic energy for light and heavy particles . . . . .	7
---	---	---

# 1 Introduction

Utilizing the Python version 3.9.13 programming language, a data-driven simulation of a 2D gas confined within a rectangular container was undertaken. The simulation was structured in accordance with the guidelines provided in the assignment file, with unique modifications implemented to address specific problems. To maximize computational efficiency, the code was developed using array-based methodologies, specifically utilizing the Numpy library. By circumventing the use of for-loops, the simulation speed was significantly enhanced. This report details the framework of the written code and presents the solutions developed for each task outlined in the assignment file.

# 2 Code framework

In order to facilitate the simulation of each problem, two Python files were created to handle the initialization of circles (including position, angle, and velocity) while ensuring no overlap with the walls or other particles. These files also contained all necessary functions for collision detection with both the horizontal and vertical walls, as well as between two particles. Additional functionality included calculating new positions and velocities after each collision, finding all possible collisions, and storing velocity magnitudes for each particle throughout the simulation. To optimize the simulation speed, for-loops were avoided and instead, an array-based approach was adopted. For each problem, a dedicated Python file was created to demonstrate the code structure. Finally, a separate Python file was developed to plot the results of each problem as requested.

# 3 Simulation results

This section provides an in-depth presentation of the simulation results for each problem. To gain insights into the various phenomena under different conditions, unique parameters were chosen for each problem. Each problem's specific parameters are thoroughly detailed to provide a comprehensive understanding of the simulation outcomes.

## 3.1 Problem 1

The simulation was conducted for two different particle numbers (2,000 and 4,000) until a total of 40,000 collisions were reached, with an initial velocity of 5 m/s. The mass and radius of the particles were chosen as 0.002 and 0.001 of their respective units, respectively. Therefore, the simulation was repeated for two different states as mentioned above.

The results, the velocity distribution, are depicted in Figure 1 and Figure 2. These figures show the velocity distribution in five snapshots, including the initial velocity and after 10k, 20k, 30k, and 40k collisions. A histogram was used to effectively analyze the velocity distribution. Figure 3 shows the velocity distribution based on the 2D Maxwell-Boltzmann distribution at different temperatures. It can be observed that the distribution is temperature-dependent, with lower temperatures resulting in taller and narrower distributions.

As the number of collisions increases, the velocity distribution in Figure 1 and Figure 2 gradually approaches the Maxwell-Boltzmann distribution, indicating that the speed distribution for the 2D gas is similar to the Maxwell-Boltzmann distribution as it approaches equilibrium. Comparing Figure 2 and Figure 3, it can be inferred that a greater number of particles result in a smoother and better velocity distribution. In other words, Figure 2 displays a smoother distribution of particles compared to Figure 1, which represents 2,000 particles. However, Figure 1 suggests that the system needs more collisions to reach equilibrium

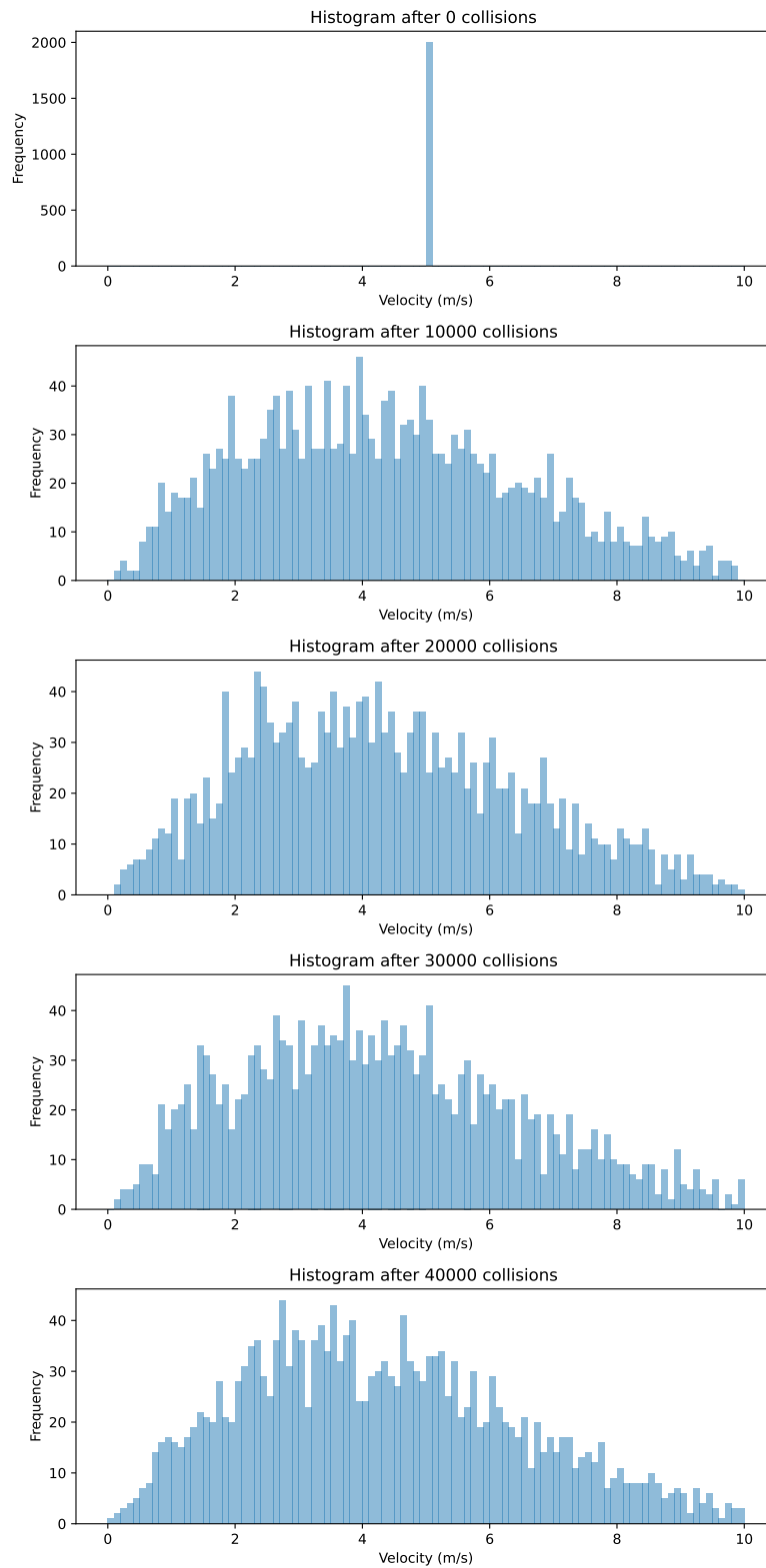


Figure 1: Histogram of speed distribution for 40,000 collisions between 2,000 particles.

### 3.2 Problem 2

In this problem, the impact of different particle masses is investigated in the velocity distribution of particles. The particles had a radius and an initial mass ( $m_0$ ) of 0.001 each. To comply with the

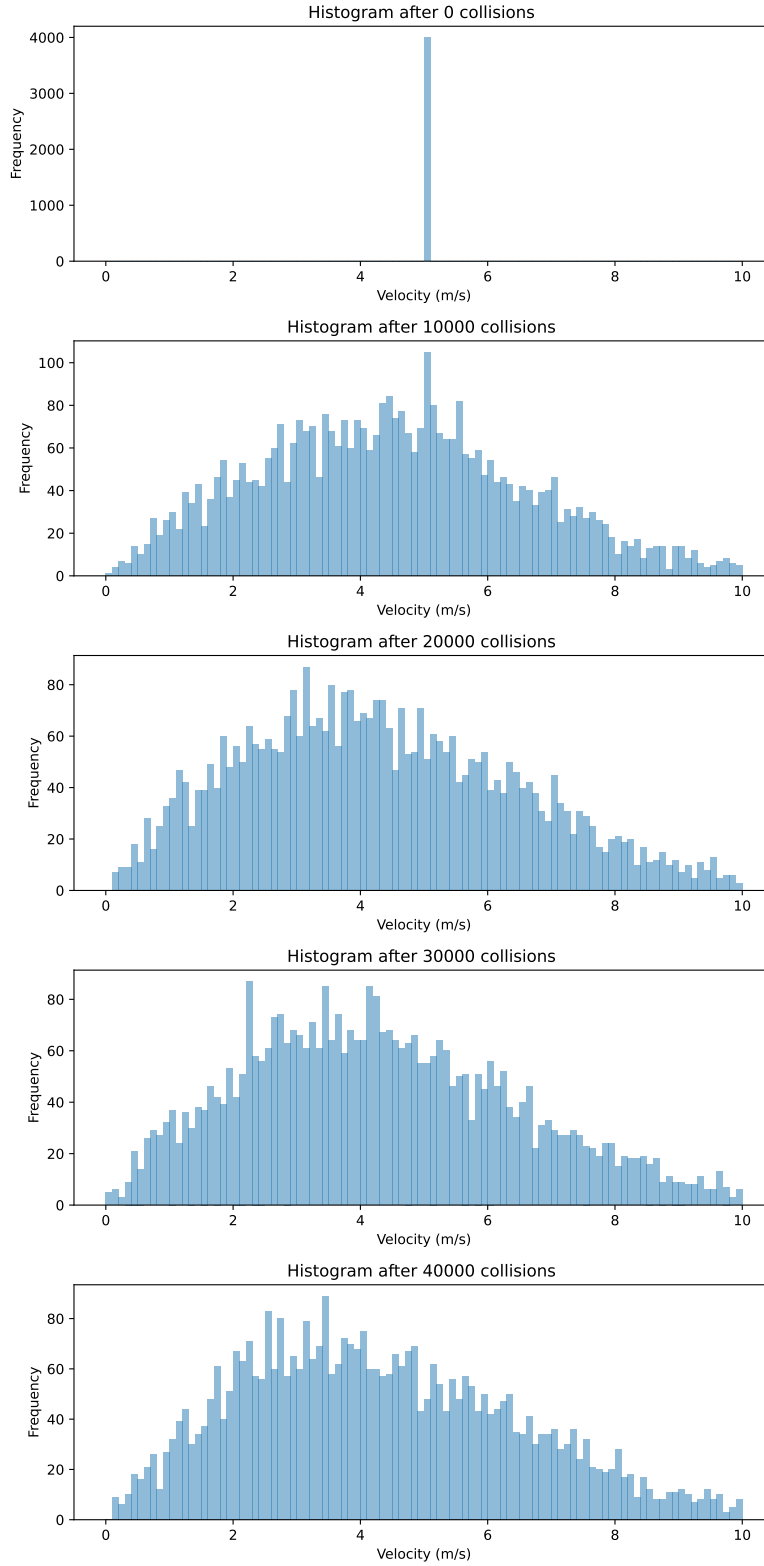


Figure 2: Histogram of speed distribution for 40,000 collisions between 4,000 particles.

problem requirements, half of the particle masses were assigned to  $m = 4m_0$ , and 60,000 collisions were simulated among 4,000 particles.

The histograms of the velocity distribution for particles with masses  $m = m_0$  and  $m = 4m_0$  are shown in Figures 4 and 5, respectively. Figures demonstrate that over time, the velocity

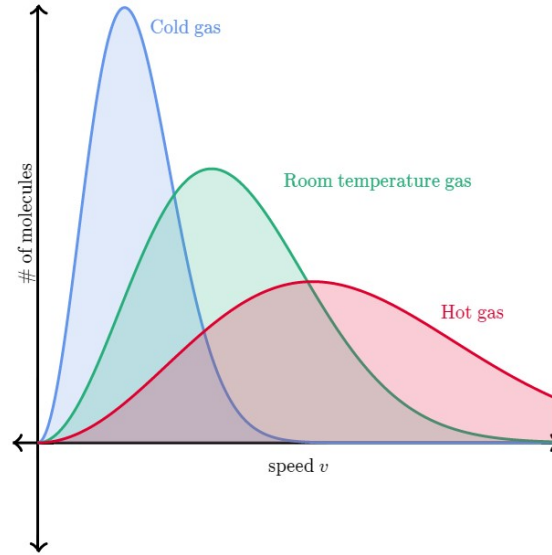


Figure 3: Maxwell-Boltzmann distribution for different temperatures (Akademi 2023).

distribution of heavier particles decreases, ultimately reaching an equilibrium with the lighter particles. The majority of heavy particles have a velocity less than the initial velocity, whereas the velocity distribution of lighter particles is mostly above the initial velocity.

The observed behavior of velocity distribution can be considered evidence of energy conservation in the absence of energy loss ( $\zeta = 1$ ). The average velocity for both particles and total kinetic energy were also calculated for both the initial and equilibrium states which can be reached at Table 1. The difference in the average kinetic energy between the two states was found to be minimal (0.00001), which can be attributed to precision errors in the velocity calculation.

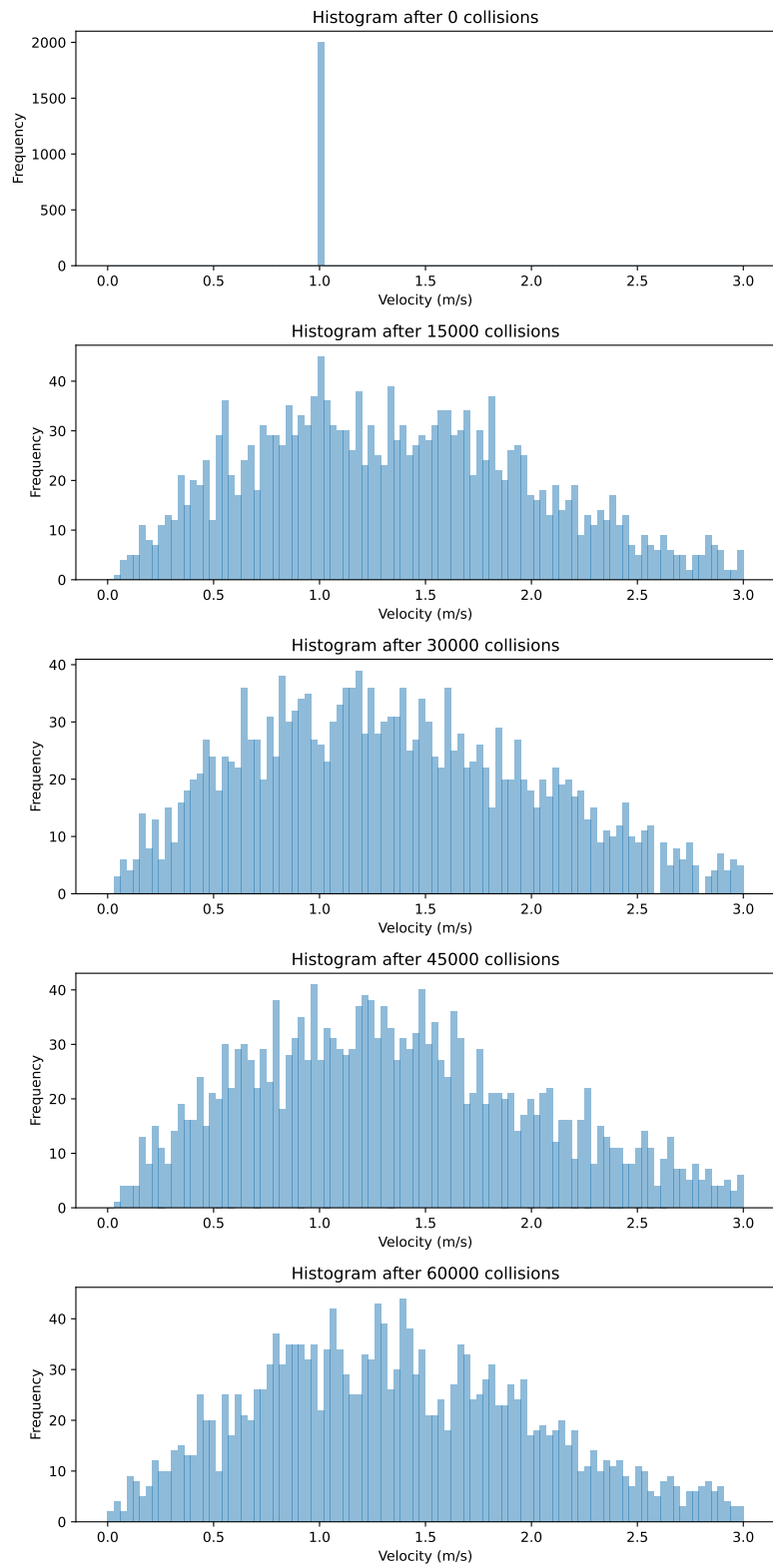


Figure 4: Histogram of speed distribution for 60,000 collisions for particles with  $m = m_0$ .

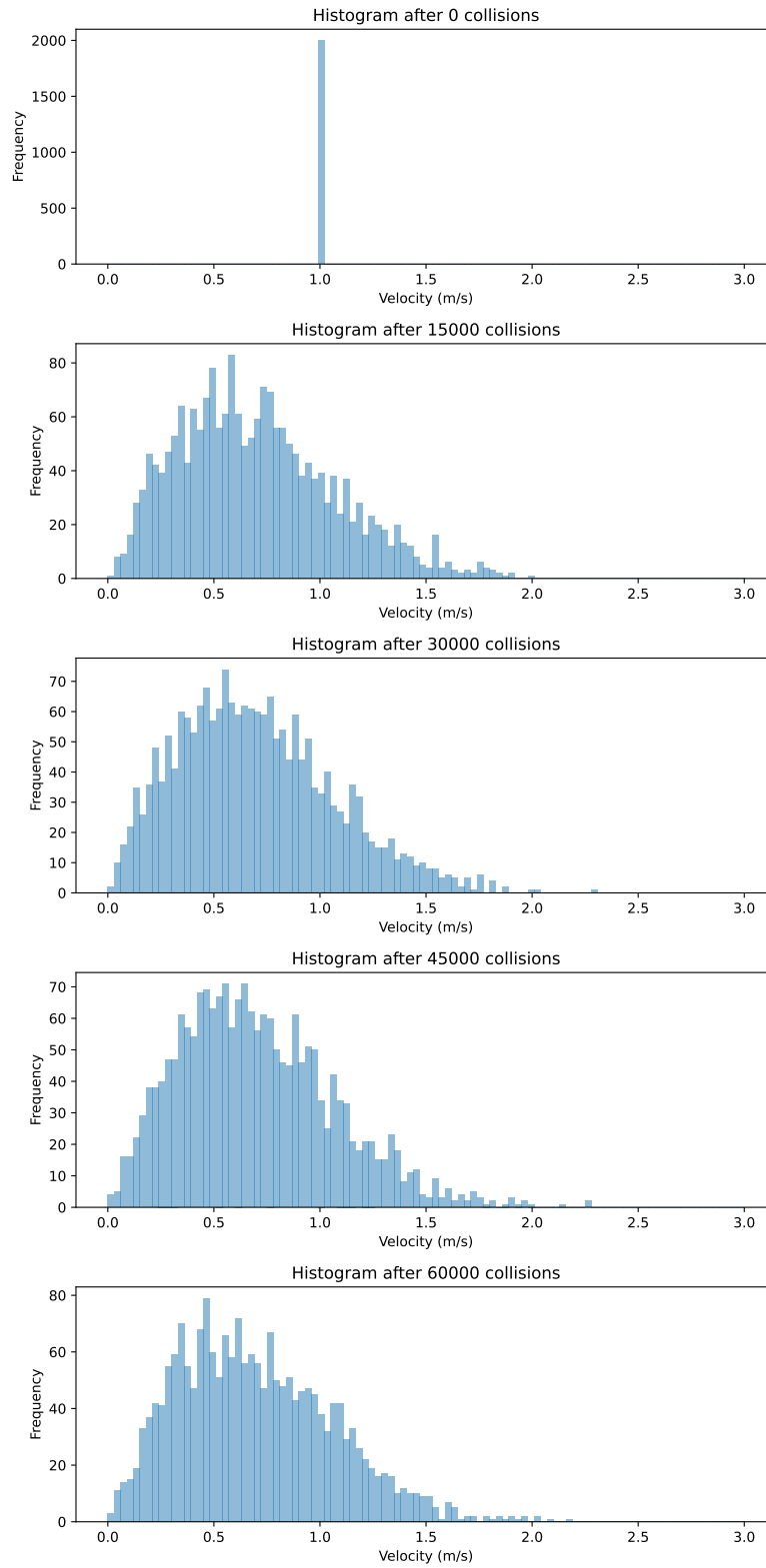


Figure 5: Histogram of speed distribution for 60,000 collisions for particles with  $m = 4m_0$ .

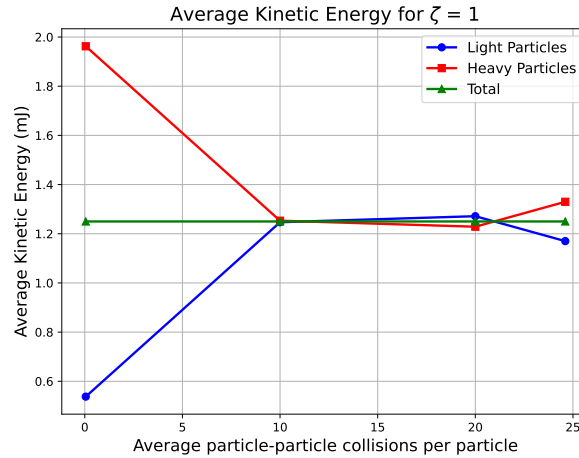


Table 1: Average velocity and kinetic energy for light and heavy particles

States	Average Velocity for Light Particles (m/s)	Average Velocity for Heavy Particles (m/s)	Average Kinetic Energy for Light Particles (mJ)	Average Kinetic Energy for Heavy Particles (mJ)
Initial	1.0000	1.0000	0.500	1.258
Equilibrium	1.4122	0.6983	2.000	1.242

### 3.3 Problem 3

To initiate the discussion of this problem, it is important to define the criterion for a low average number of particle-particle collisions per collision. Therefore, a value of less than 0.1 was considered low, and a value of 0.05 was chosen for the simulation. The simulation was then carried out to determine the time period at which the average number of collisions per particle reached 117 for  $\zeta = 1$ . This point was used as the initial point for the final plot. Similar ratios were obtained for different restitution coefficients ( $\zeta$ ), and the results were plotted in Figures 6, 7 and 8. As depicted in Figure 6, the total energy of the system remained constant over time. However, energy was transferred between the heavy and light particles over time. In contrast, Figures 7 and 8 show that the average kinetic energy of particles (both light and heavy) and the average total kinetic energy decreased over time. This can be attributed to the decrease in the restitution coefficient ( $\zeta$ ), which leads to energy loss during collisions. In other words, as the restitution coefficient decreases, the system reaches a stationary state sooner.

Figure 6: Average kinetic energy for light and heavy particles over the time ( $\zeta = 1$ )

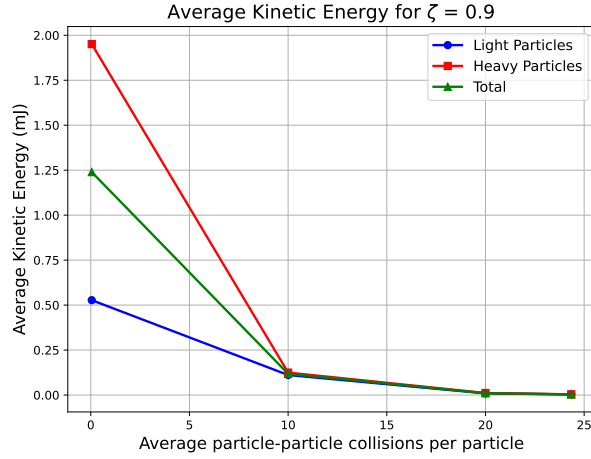


Figure 7: Average kinetic energy for light and heavy particles over the time( $\zeta = 0.9$ )

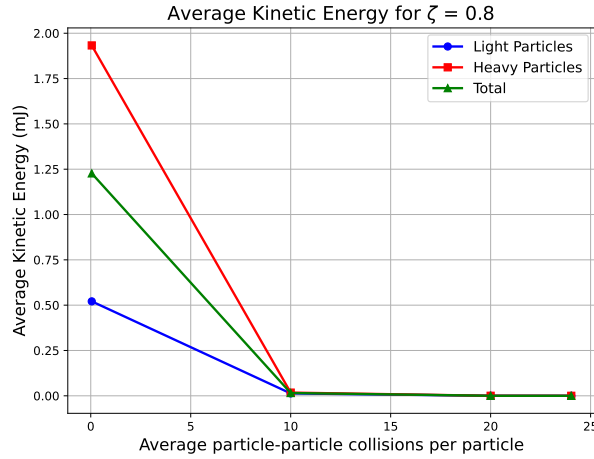


Figure 8: Average kinetic energy for light and heavy particles over the time( $\zeta = 0.8$ )

### 3.4 Problem 4

To set the initial positions of all particles (except for the big particle), the random uniform function argument was adjusted to half of the system size. The radius of the smaller particles was set to 0.008, and to occupy slightly over 50% of the half square, 1300 particles were required. The values for mass, restitution coefficient ( $\zeta$ ), and initial velocity were assigned as 0.001, 0.5, and 5, respectively.

Once the system reached 10% of its initial energy, the position of all particles was stored for further analysis. The initial velocity was then varied between 2.75 and 5 in increments of 0.25 to investigate its effect on the size of the crater formed during the simulation. To measure size of the crater, it can be referred to the position of big particle meaning the depth of the crater. on the other hand, the maximum size of the crater around the center of the square can be measure by finding the last position of the particle and their distance with  $x = 0.5$ . Then, it can be sorted and find the ones which are in the same height. Figure 9 shows the changes of depth of the crater vs initial velocity. As it can be seen in the figure, depth of the crater will increase when the initial velocity increases.

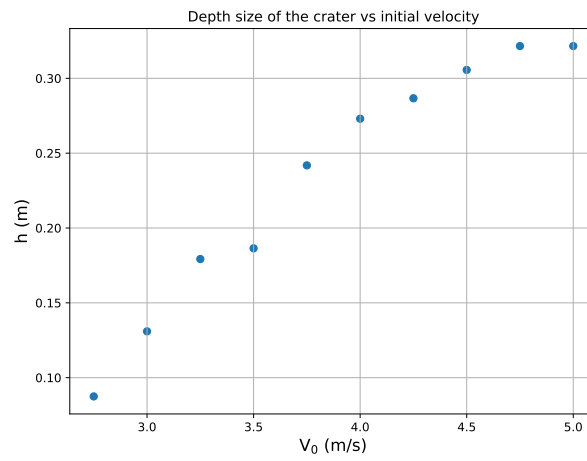


Figure 9: Depth size of the crater vs initial velocity

## Bibliography

Akademi, Khan (2023). *What is the Maxwell-Boltzmann distribution?* 2023. URL: <https://www.khanacademy.org/science/physics/thermodynamics/temp-kinetic-theory-ideal-gas-law/a/what-is-the-maxwell-boltzmann-distribution>.

## Appendix

### A Code structure